Human Molecular Genetics, 2005, Vol. 14, No. 4 ***513–524***
doi:10.1093/hmg/ddi048
Advance Access published on January 7, 2005

CECR2, a protein involved in neurulation, forms a novel chromatin remodeling complex with SNF2L

Graham S. Banting[1,†,‡], Orr Barak[2,†], Tanya M. Ames[1], Amanda C. Burnham[1], Melanie D. Kardel[1], Neil S. Cooch[2], Courtney E. Davidson[1], Roseline Godbout[3], Heather E. McDermid[1,*] and Ramin Shiekhattar[2]

[1]Department of Biological Sciences, University of Alberta, Edmonton, Alberta T6G 2E9, Canada, [2]The Wistar Institute, 3601 Spruce Street, Philadelphia, PA 19104, USA and [3]Cross Cancer Institute, Edmonton, Alberta T6G 1Z2, Canada

Received September 18, 2004; Revised December 15, 2004; Accepted December 21, 2004

Chromatin remodeling complexes play critical roles in development. Here we describe a transcription factor, CECR2, which is involved in neurulation and chromatin remodeling. *CECR2* shows complex alternative splicing, but all variants contain DDT and bromodomain motifs. A mutant mouse line was generated from an embryonic stem cell line containing a genetrap within *Cecr2.* Reporter gene expression demonstrated *Cecr2* expression to be predominantly neural in the embryo. Mice homozygous for the *Cecr2* genetrap-induced mutation show a high penetrance of the neural tube defect exencephaly, the human equivalent of anencephaly, in a strain-dependent fashion. Biochemical isolation of CECR2 revealed the presence of this protein as a component of a novel heterodimeric complex termed CECR2-containing remodeling factor (CERF). CERF comprises CECR2 and the ATP-dependent chromatin remodeler SNF2L, a mammalian ISWI ortholog expressed predominantly in the central nervous system. CERF is capable of remodeling chromatin *in vitro* and displays an ATP hydrolyzing activity that is stimulated by nucleosomes. Together, these data identify a novel chromatin remodeling complex with a critical role in neurulation.

INTRODUCTION

Chromatin remodeling, the alteration of DNA–histone contacts and nucleosome positioning, can result from covalent histone modification or ATP-dependent protein complexes that reposition nucleosomes on the DNA strand (reviewed in 1,2). A wide range of cellular processes, such as transcription, replication and repair, rely on modification of chromatin, and as such several examples of human disease are associated with various chromatin remodeling proteins (reviewed in 3,4).

Recently, research has garnered some insight into the role of ATP-dependent chromatin remodelers in development. For example, neural and hematopoietic development in humans requires the ATRX remodeler (5,6). In addition, mice mutated for the PASG remodeler demonstrate premature aging and growth retardation (7). Finally, *Drosophila* with a mutated NURF remodeling factor exhibit homeotic transformations and melanotic tumors (8).

Many of the human chromatin remodeling proteins were first identified and studied in model organisms such as flies and yeast. *Drosophila* ISWI is a member of the ATP-dependent family of chromatin remodelers and has been well characterized (8,9). ISWI is a core member of at least three separate chromatin remodeling complexes in *Drosophila*, which include NURF (nucleosome remodeling factor, 10), ACF (ATP-utilizing chromatin assembly and remodeling factor, 11) and CHRAC (chromatin assembly complex, 12).

In mammals, two homologs of *Drosophila* ISWI exist, *SNF2H* and *SNF2L* (13–15). Developmentally, *Snf2h* and *Snf2l* have been shown to have distinct expression patterns during embryogenesis. However, both are expressed in neural tissues, with *Snf2h* being predominantly associated with proliferating neurons while *Snf2l* is associated with terminally differentiated neurons (14). *Snf2h* knockouts are peri-implantation lethal, with defects in ES cell proliferation (16). An *Snf2l* knockout has not yet been described.

SNF2H has been shown biochemically to possess ATPase activity, and like its *Drosophila* homolog, is present in various protein complexes, including WCRF/hACF (William syndrome transcription factor related remodeling factor, 17),

*To whom correspondence should be addressed. Tel: +1 7804925377; Fax: +1 7804929234; Email: hmcdermi@ualberta.ca
†The authors wish it to be known that, in their opinion, the first two authors should be regarded as joint First Authors.
‡Present address: Department of Medical Genetics, University of Alberta, Edmonton, Alberta T6G 2H7, Canada.

RSF (remodeling and splicing factor, 18), WICH (WSTF-ISWI chromatin remodeling complex, 19), NoRC (nucleolar remodeling complex, 20), huCHRAC (chromatin accessibility complex, 21) and SNF2H-cohesin (22). Recently, the first mammalian SNF2L-containing complex, human NURF (hNURF), was identified and characterized (23). hNURF possesses ATP-dependent chromatin remodeling activity and regulates *engrailed-1* (*en-1*) and *engrailed-2* (*en-2*) expression. On the basis of *engrailed* function in mid-hindbrain development (24,25), it has been postulated that hNURF is important for neuronal development (14,23).

We report the purification and characterization of a second SNF2L-containing complex, CERF (CECR2-containing remodeling factor). Along with SNF2L, this heterodimeric complex contains *CECR2* (cat eye syndrome chromosome region, candidate 2), a gene previously identified as being in the chromosome 22q11 region duplicated in the human disorder cat eye syndrome (26). This syndrome is characterized by defects of the eye, heart, anus, kidney, skeleton, face and mental development; however the neural tube develops normally. Here we show that a genetrap-induced mutant allele of mouse *Cecr2* is associated with the neural tube defect (NTD) exencephaly in a strain specific manner. Although the role of overexpression of *CECR2* in CES remains unclear, our mutation of *Cecr2* produces a mouse model for the human NTD anencephaly (equivalent of exencephaly in mice). CECR2/Cecr2 contains both a DDT motif and bromodomain, typical of proteins involved in chromatin remodeling. The CERF complex has intrinsic nucleosome-dependent ATPase activity and remodels chromatin in an ATP-dependent fashion. Snf2l has previously been speculated to have a role in neurogenesis (14), and the observation that one of its binding partners is associated with an NTD lends further evidence to this hypothesis.

RESULTS

CECR2/Cecr2 codes for a putative transcription factor

We previously identified the novel bromodomain-containing gene, *CECR2* (26) (GenBank accession no. Q9BXF3), during the process of gene mapping in the cat eye syndrome critical region on chromosome 22q11.2. To further characterize *CECR2*, we used RT–PCR, RACE and *in silico* approaches to identify the complete gene structure (Fig. 1A). *CECR2* was determined to contain 19 exons producing an open reading frame of 4392 bp, which encodes a 1464 amino acid predicted protein. Four separate polyadenylation sites exist and are represented by EST clones. Exon 19 has three distinct polyadenylation locations producing exon 19 variants that are 1111, 1307 or 5313 nucleotides in length. These do not affect the size of the final protein, as exon 19 is, with the exception of a single codon, entirely untranslated. These polyadenylation sites are conserved in mouse. A fourth 3′ end was identified in exon 13; this creates a transcript in which exon 13 is not spliced to exon 14. Instead this transcript extends into intron 13, which results in six additional amino acids being added to exon 13. This is followed by a short 50 nucleotide 3′-UTR. The resulting 2 kb transcript encodes the CECR2b protein (GenBank accession no. AAL07393, 27) consisting of 506 amino acids. To date, *CECR2b* has not been identified in mouse. The protein sequence of CECR2/Cecr2 contains a number of domains consistent with an ISWI-associated protein including DDT, AT-hook and a bromodomain (Fig. 1A). Importantly, the DDT domain is present in virtually all known ISWI binding partners and was shown to be necessary for ISWI binding in *Drosophila* ACF1 (28). Bromodomains have been defined through structural and functional studies as acetyl-lysine residue binding domains (reviewed in 29). Lysine acetylation is a modification often found in histone tails (30,31) and is associated with active chromatin. A putative nuclear localization signal is found in exon 5. Interestingly, all five of the amino acid motifs are found within the first 13 exons, and thus, are shared between *CECR2* and *CECR2b.* There are no recognizable motifs/domains within the remaining two-thirds of CECR2/Cecr2, and the function of this portion of the protein is unclear.

It also became apparent that other *CECR2* transcript variants existed due to alternative splicing. On the basis of the RT–PCR results using cDNA synthesis primers in the 3′-UTR of exon 13 or 19, we were able to identify transcripts that alternatively removed exons 2–7, 2–8, 4–7, 4–8 or 8 alone (Fig. 1A). These variants were found in *CECR2, CECR2b* and in mouse *Cecr2.* In addition, exons 14 and 16 also contain alternative splice sites which yield smaller variants of those exons. Owing to the large size of *CECR2*, we were unable to determine, by RT–PCR, in which combinations the exon 14 and 16 splicing events were found with the exon 2–8 events, or alternative 3′ polyadenylation events. All splicing events maintained the open reading frame, and were found in mouse *Cecr2* (except exon 13′), which suggests biological relevance. *CECR2* exons 1–10, which contain portions that are common to all theoretical transcripts, were used as a probe on a northern blot (data not shown). Predominant transcripts of 10, 9.5 and 6.0 kb were observable in many human tissues. The 10 and 9.5 kb transcripts were abundant in adult liver, but absent in fetal liver. They were also seen in fetal brain, lung and kidney, as well as adult heart, brain, placenta, lung, liver, skeletal muscle and pancreas, while being low or absent in adult spleen, thymus, prostate, small intestine, colon and leukocytes. The 6.0 kb transcript was faint in many tissues but only showed strong hybridization in testis, along with the 9.5 kb transcript. Only the 10 kb transcript was seen in ovary. The bands of 10, 9.5 and 6.0 kb likely correspond to transcripts containing exons 1–19″, 1–3 + 8/9–19″ and 1–19/19′, respectively. The size difference of many of the splice variants is small, thus they are likely not resolvable on the northern blot. Interestingly, *CECR2b* was not seen on these northern blots at 2 kb. It is likely expressed at a level not detectable by northern hybridization, as it can be amplified from various tissues by RT–PCR (data not shown).

Generation of Cecr2 mutant mice

BLAST analysis of the *CECR2* cDNA identified a 5′ RACE product from the mouse ES cell line CT45, containing the genetrap pGT1 (32). Since we were interested in *CECR2* as a possible dosage sensitive gene in the CES duplicated region,

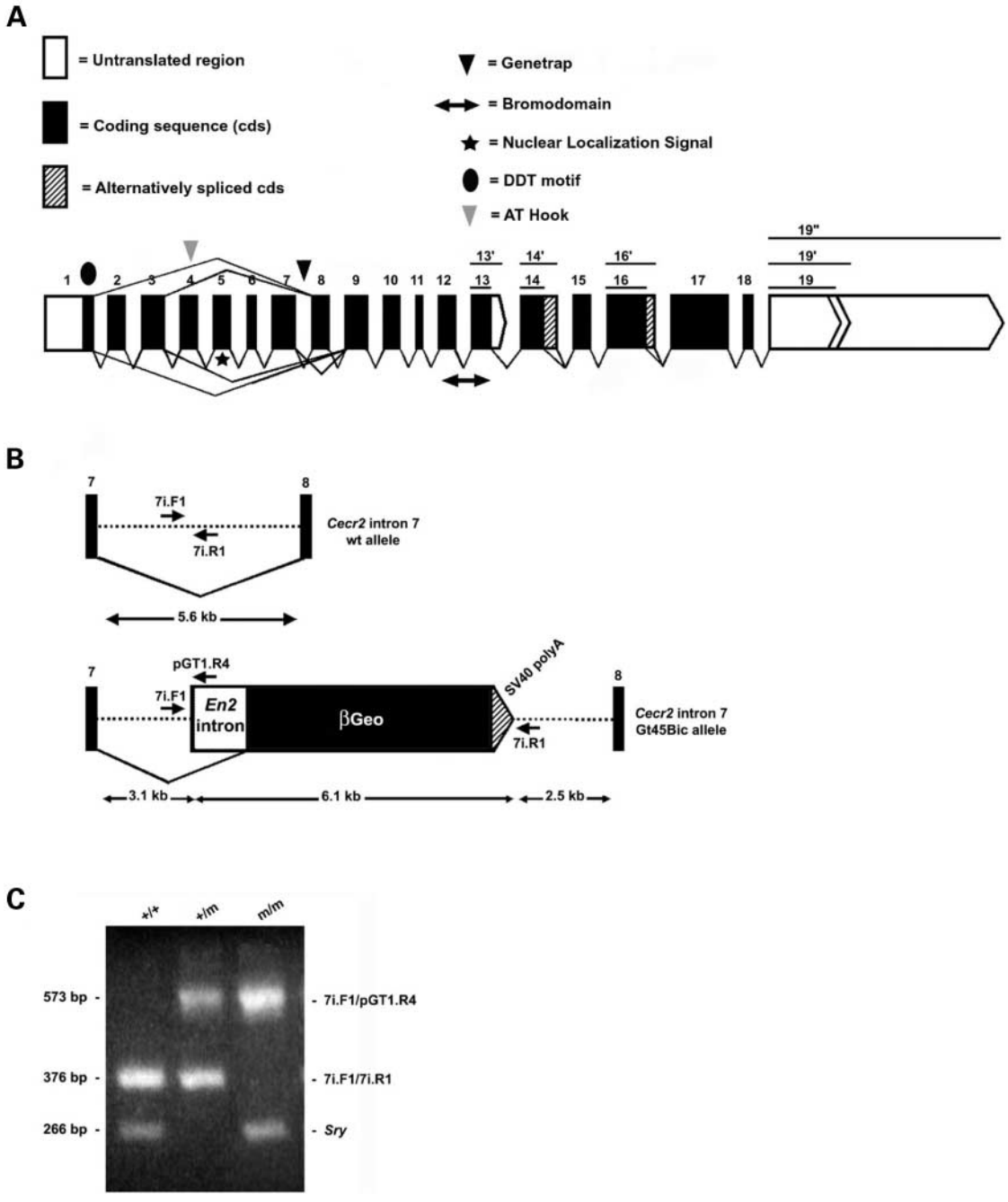

Figure 1. (**A**) Structure of *CECR2/Cecr2*. Shown are locations of CECR2/Cecr2 amino acid motifs and the location of the genetrap insertion within *Cecr2* (black arrow). Exon 13′ is found only in humans. (**B**) Generation of *Cecr2* mutant mice. Structure of the *Cecr2* β-Geo genetrap allele. Positions of the genotyping primers are noted. (**C**) An example of a *Cecr2* genotyping PCR. *Sry* primers were used to determine the sex of the animals.

we reasoned that a genetrap mutation might be informative in the understanding of CES. The sequence of the CT45 5′ RACE product corresponded to exon 7 of *Cecr2*, suggesting that the genetrap fell within intron 7 or 8 (due to potential alternative splicing of exon 8) of *Cecr2*. The pGT1 insertion was mapped to the middle of intron 7 (Fig. 1B), and a PCR assay for genotyping was designed (Fig. 1C). The 129P2/Ola-derived CT45 ES cells were used to generate a male mouse chimera, which was mated to BALB/c females to generate F_1 animals on a mixed 129P2/BALB background. The mutant allele was designated $Cecr2^{Gt45Bic}$. F_1 heterozygotes were intercrossed to produce a total of 533 progenies. On the basis of genotype totals, it was clear that $Cecr2^{Gt45Bic}$ homozygotes were not represented in the appropriate Mendelian ratio. Of 533 pups genotyped at weaning, 170 were wild-type (32%), 323 were heterozygotes (60%) and only 40 (7.5%) were homozygous for $Cecr2^{Gt45Bic}$. Collection of fetuses at 19 days suggested that the remaining

Cecr2$^{Gt45Bic/Gt45Bic}$ pups were dying perinatally (discussed subsequently). Strikingly, the 7.5% of *Cecr2*$^{Gt45Bic/Gt45Bic}$ mice that were weaned and genotyped were indistinguishable from their wild-type and heterozygous littermates, and proved to be fertile.

To confirm that only one genetrap insertion was present in the CT45 ES cell line, we probed a Southern blot to compare five restriction enzyme digests of ES cell and homozygous mouse mutant DNA, using a probe within the genetrap. The single bands revealed for each enzyme were consistent with a single insertion (data not shown).

Cecr2$^{Gt45Bic/Gt45Bic}$ mice develop NTDs

In order to identify the etiology of the perinatal lethality, we characterized embryos [9.5–19.5 days post-coitus (dpc)] from 129P2/BALB *Cecr2*$^{+/Gt45Bic}$ intercrosses. We observed a high rate of the NTD exencephaly in embryos homozygous for the genetrap (Fig. 2A). Exencephaly results from failure of neural tube closure in the midbrain region beginning at ~8.5 dpc and is the equivalent to human anencephaly (33). Mendelian ratios of the three genotypes obtained were close to those expected (Table 1), suggesting that exencephaly was the likely cause of perinatal death, followed by cannibalization by the mother. The only additional phenotype observed was a lack of eyelids observed in some homozygous mutant embryos (Fig. 2A), which is also seen in some other forms of exencephaly (34,35). No features overtly similar to CES, particularly coloboma, were noted. Exencephaly was observed at a frequency of 67% in *Cecr2* homozygotes in 129P2/BALB animals, and also at a low frequency (3.5%) in *Cecr2* heterozygotes (Table 1).

Cecr2 expression is concentrated in the nervous system

We utilized the *LacZ* reporter gene within the pGT1 genetrap to characterize the expression profile of *Cecr2* during development. Driven by the native *Cecr2* promoter, X-gal staining of the Cecr2–LacZ fusion protein should yield a good representation of Cecr2 protein distribution. We stained *Cecr2* heterozygotes and homozygotes from ages 9.5 to 13.5 dpc (Fig. 2). At 10.5 dpc, Cecr2 is weakly localized throughout most of the embryo with high concentrations in the recently closed neural tube (Fig. 2B). In homozygous embryos with exencephaly at 9.5 dpc, Cecr2 expression is high at the margins of the neural folds that have failed to fuse (Fig. 2C). High concentrations of Cecr2 are also found in the rostral portion of the brain, along with the pharyngeal arches (Fig. 2D). There is a noticeable lack of Cecr2 in the heart and liver.

By 13.5 dpc, the neural enrichment of Cecr2 is even more pronounced. The staining of the 13.5 dpc homozygote (Fig. 2E) is similar to that of the heterozygote (Fig. 2F) with the exception of the homozygous exencephalic brain, which stains strongly throughout. There is, however, a noticeable concentration of Cecr2 in the limb mesenchyme in both genotypes. To determine whether any skeletal defects were present in *Cecr2* mutant mice, we stained embryos with the cartilage-specific dye Alcian blue (Fig. 2G). All three genotypes were examined, and the only observable difference among the three was the obvious lack of a forming cranium in the exencephalic *Cecr2* homozygous animals, which is considered a defect secondary to exencephaly (36).

Sectioning of X-gal stained embryos confirmed the *Cecr2* fusion gene localization throughout the nervous system (Fig. 3A), including the neural tube and adjacent spinal ganglia (Fig. 3B). Staining was also seen in the mesenchyme of the forming limbs, nasal epithelium (Fig. 3B), in the lens and neuroretina of the forming eye (Fig. 3C) and in the intercostal mesenchyme (Fig. 3D).

Cecr2-associated exencephaly is strain dependent

For reasons unrelated to this work, the FVB/N strain background was introduced into the mixed 129P2/BALB *Cecr2* animals. The FVB/N background reduced the penetrance of *Cecr2* induced exencephaly from 67 to 36% (Table 1). Due to this observation, we decided to move the *Cecr2*^{Gt45Bic} mutation onto the BALB/c, 129P2/Ola and FVB/N strain backgrounds. By backcrossing to the pure strain for at least five generations (F_5) we generated incipient congenic lines for BALB/c, 129P2/Ola and FVB/N. At F_5 or F_6 *Cecr2*^{Gt45Bic} heterozygotes were then intercrossed and embryos collected for analysis. Exencephaly penetrance in the BALB/c background (74%) was higher than that of the 129P2/BALB mixed background. Penetrance in the 129P2/Ola background was 63%. Surprisingly, on the FVB/N background exencephaly penetrance was reduced to zero. Interstrain differences are seen in other genes associated with exencephaly (37,38). When BALB/c *Cecr2*^{Gt45Bic} heterozygous males were crossed with non-penetrant FVB/N *Cecr2*^{Gt45Bic} homozygous females, exencephaly reappeared, but in a very small proportion of resulting embryos (one in 35 homozygous mutant embryos). These experiments therefore suggest the presence of a semi-dominant or dominant modifier locus (or loci) in the FVB/N strain.

Isolation of a novel SNF2L complex containing CECR2

We have established that Cecr2 plays a role in neurulation. Analysis of CECR2 interacting proteins could give insight into CECR2 function. The DDT, BAZ and bromodomain motifs found in CECR2/Cecr2 suggest its incorporation in an ISWI family chromatin remodeling complex, as nearly all ISWI binding proteins share these motifs (17,23,39,40). Furthermore, the CNS expression of Cecr2 in transgenic mouse led us to ask whether Cecr2 bound to the neuronally expressed Snf2l ISWI family remodeler (14). In a previous study on SNF2L, we subjected nuclear extracts to gel filtration chromatography and noted the presence of a larger molecular weight (~1 MDa) and smaller molecular weight (~600 kDa) SNF2L-containing fractions (23). We purified the larger SNF2L-containing complex to homogeneity resulting in the isolation of hNURF. We now hypothesized that the, as yet uncharacterized, smaller weight SNF2L complexes may incorporate CECR2.

To characterize the smaller molecular weight SNF2L-associated complexes, we subjected bulk, unfractionated nuclear extract from Flag-SNF2L HEK293 cells to Flag immunoaffinity purification. The beads were washed extensively,

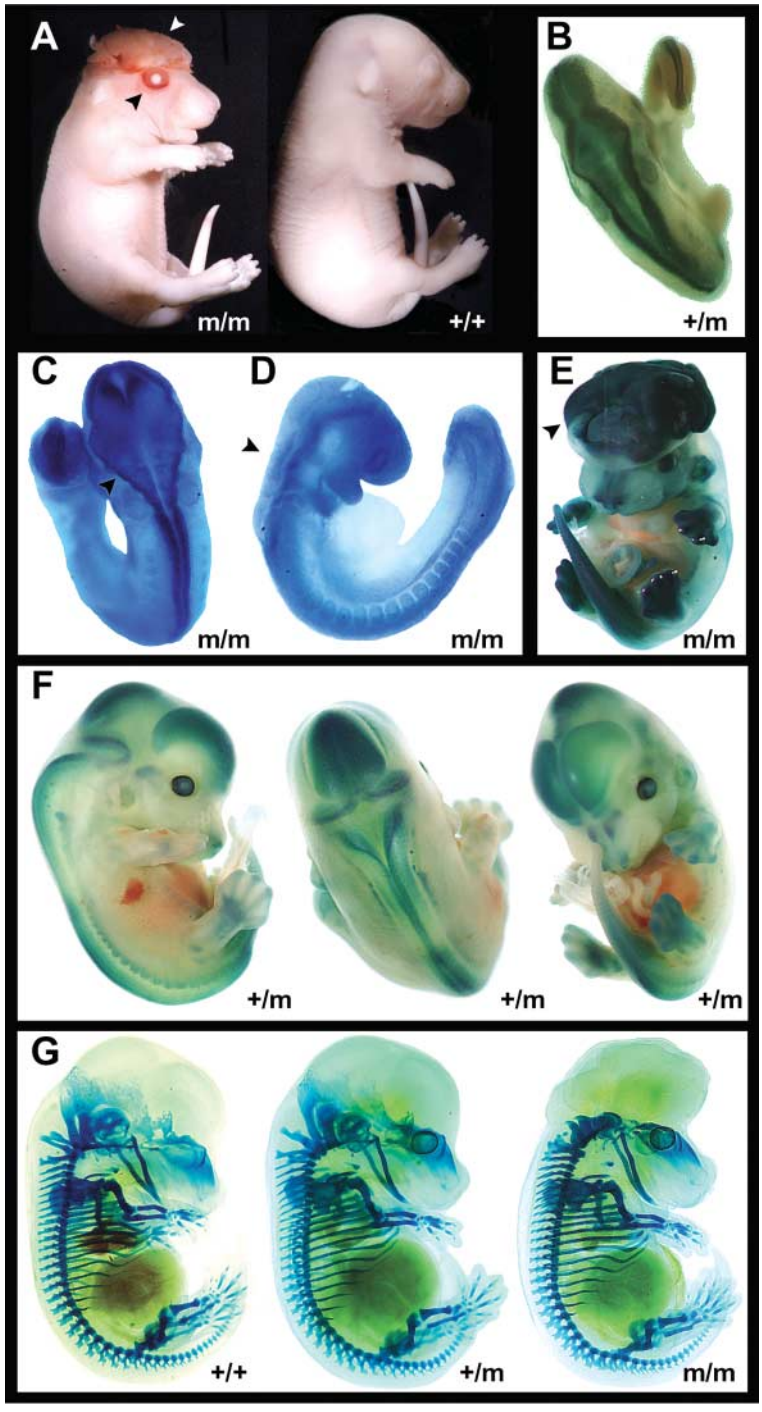

Figure 2. Phenotypes of *Cecr2* mutant mice, and expression patterns of *Cecr2*. (**A**) Phenotype of $Cecr2^{Gt45Bic}$ ('m') mutant mice; 19.5 dpc $Cecr2^{Gt45Bic/Gt45Bic}$ and wild-type (+/+) fetuses. *Cecr2* mutant mice show the NTD exencephaly (white arrow) at high penetrance. Eyelids are missing in some mutant animals (black arrow). (**B**) A 10.5 dpc $Cecr2^{+/Gt45Bic}$ embryo stained with X-gal, showing *Cecr2* fusion protein localization in a recently closed neural tube. (**C** and **D**) Two views of a 9.5 dpc exencephalic $Cecr2^{Gt45Bic/Gt45Bic}$ embryo stained with X-gal. *Cecr2* expression is concentrated at the leading edge of the neural folds which have failed to fuse in the midbrain region (arrow). A wild-type littermate showed no staining (data not shown). (**E**) A 13.5 dpc $Cecr2^{Gt45Bic/Gt45Bic}$ animal, stained with X-gal, showing exencephaly (arrow). Note staining of exencephalic brain tissue. (**F**) Three views of a 13.5 dpc $Cecr2^{+/Gt45Bic}$ embryo stained with X-gal. By 13.5 dpc, *Cecr2* expression is highly concentrated in the nervous system, with some expression in the nasal epithelium and limb mesenchyme. (**G**) 14.5 dpc *Cecr2* embryos of three different genotypes stained with a cartilage-specific dye. The only abnormality is the lack of a forming cranium in the exencephalic $Cecr2^{Gt45Bic/Gt45Bic}$ embryo. All embryos in Figure 2 are on a BALB/129 background.

Table 1. Penetrance of exencephaly is variable depending upon mouse genetic background

	BALB/129P2			BALB/129P2/FVB			FVB/N[a]			BALB/c[a]			129P2/Ola[a]		
Genotype	*m*/*m*[b]	+/*m*	+/+	*m*/*m*	+/*m*	+/+	*m*/*m*	+/*m*	+/+	*m*/*m*	+/*m*	+/+	*m*/*m*	+/*m*	+/+
Exencephaly	24	4	0	21	7	1[c]	0	0	0	35	0	0	5	1	0
Normal	12	109	38	37	166	82	45	103	60	12	110	70	3	18	8
Penetrance (%)	67	3.5	0	36	4	1	0	0	0	74	0	0	63	5.3	0

[a]Data was collected from incipient congenic strains, mostly at generation F_6 but with some at F_5.
[b]*m* = *Cecr2*^{Gt45Bic}, + = wild-type.
[c]This is the only +/+ embryo out of 250 embryos scored that had exencephaly. No other normal embryos in any other experiments have had exencephaly. Therefore, we assume this is a sporadic event.

and SNF2L complexes were eluted using a Flag competitor peptide. We analyzed elutions by SDS–PAGE followed by silver stain or western blot analysis (Fig. 4A). As expected the components of the hNURF complex, BPTF, SNF2L and RbAP46/48, were readily identified by both silver stain and western blot. In addition, we identified two novel bands by silver stain analysis at ~160 and 180 kDa, which we called p160 and p180, respectively.

We subjected the Flag-SNF2L immunoprecipitates to gel filtration analysis using a BioSil Sec400 size exclusion column. Column fractions were separated by SDS–PAGE, and polypeptides were visualized by silver stain (Fig. 4B) and identified by western blot (data not shown). Consistent with previous observations (23), the components of the hNURF complex coelute in fractions 20–24 corresponding to a molecular weight of ~1 MDa. However, a smaller novel SNF2L-associated complex measuring ~600 kDa eluted in fractions 26–28. The second smaller complex appeared to comprise the unknown p160 and p180 polypeptides along with SNF2L, one of which may have been CECR2.

We extracted and trypsinized the p160 and p180 bands followed by protein microsequencing in order to identify the polypeptides. As predicted by our hypothesis, the p160 was identical to CECR2 (GenBank accession no. Q9BXF3). Interestingly, the p180 band was identical to RSF-1 (remodeling and spacing factor-1, GenBank accession no. NP_009123) (39,41), the large subunit of the RSF complex. These data suggested the existence of one or more 600 kDa chromatin remodeling complexes comprising some combination of SNF2L, CECR2 and RSF-1.

Characterization of the subunit composition of a novel CECR2 complex

To further characterize the CECR2-containing complex both structurally and enzymatically, we designed a one-step purification of CECR2-associated polypeptides in the absence of other SNF2L-associated complexes. This method is similar to one used for purifying hNURF (23). We cloned the open reading frame of *CECR2* with an N-terminal Flag epitope tag into a eukaryotic expression vector, and constructed a clonal HEK293 cell line stably expressing Flag-CECR2. Nuclear extract from the Flag-CECR2 cells was subjected to immunoprecipitation using anti-Flag antibodies followed by elution with a competitor Flag peptide. Elutions were analyzed by SDS–PAGE followed by silver stain and western blot analysis. Using silver stain, we noted the presence of two high molecular weight polypeptides absent in the mock IP (Fig. 5A). A western blot using antibodies raised against human SNF2L and CECR2 confirmed the identity of these polypeptides as CECR2 at 160 kDa and SNF2L at 120 kDa, respectively (Fig. 5B). The RSF-1 polypeptide was notably absent in this purification (data not shown). This strongly suggested to us that the RSF-1 isolated along with CECR2 in the SNF2L purification described earlier (Fig. 4) was likely the result of two separate SNF2L-containing complexes coeluting in similar fractions from the gel filtration column, one incorporating CECR2 and the other RSF-1. In all, our data describe a novel chromatin remodeling complex comprising a heterodimer of CECR2 and SNF2L. We named this novel complex CERF (CECR2-containing remodeling factor).

Molecular weight determination of CERF

In order to determine the molecular weight of CERF, we subjected the elutions from the Flag-CECR2 cell line immunopurification to gel filtration chromatography using a BioSil Sec400 column. Column fractions were collected and subjected to SDS–PAGE followed by silver stain and immunoblot analysis. Using molecular weight standards, we were able to calculate the CERF molecular weight. As expected, the peak CERF immunoreactivity fractionated at ~600 kDa. This was confirmed by silver stain and western blot analysis (Fig. 5C). A minor fraction of the CERF complex appears to elute in the larger molecular weight fractions; however, we believe this is due to a 'spreading' of CERF across the gel filtration column resulting in an anomalously large molecular weight.

CERF has intrinsic nucleosome-dependent ATPase activity

ISWI family chromatin remodeling complexes display a substrate stimulated ATPase activity. For most of these complexes, both DNA and nucleosomes are capable of stimulating their ATPase activity (42); however, hNURF is only responsive to nucleosomes (23). We assayed for the ability of purified CERF to hydrolyze ATP in the presence of buffer, DNA (250 ng) or nucleosomes (250 ng). We compared three concentrations of CERF under these three conditions to vehicle and mock immunoprecipitation in order to demonstrate the specificity of this activity (Fig. 6A). As expected,

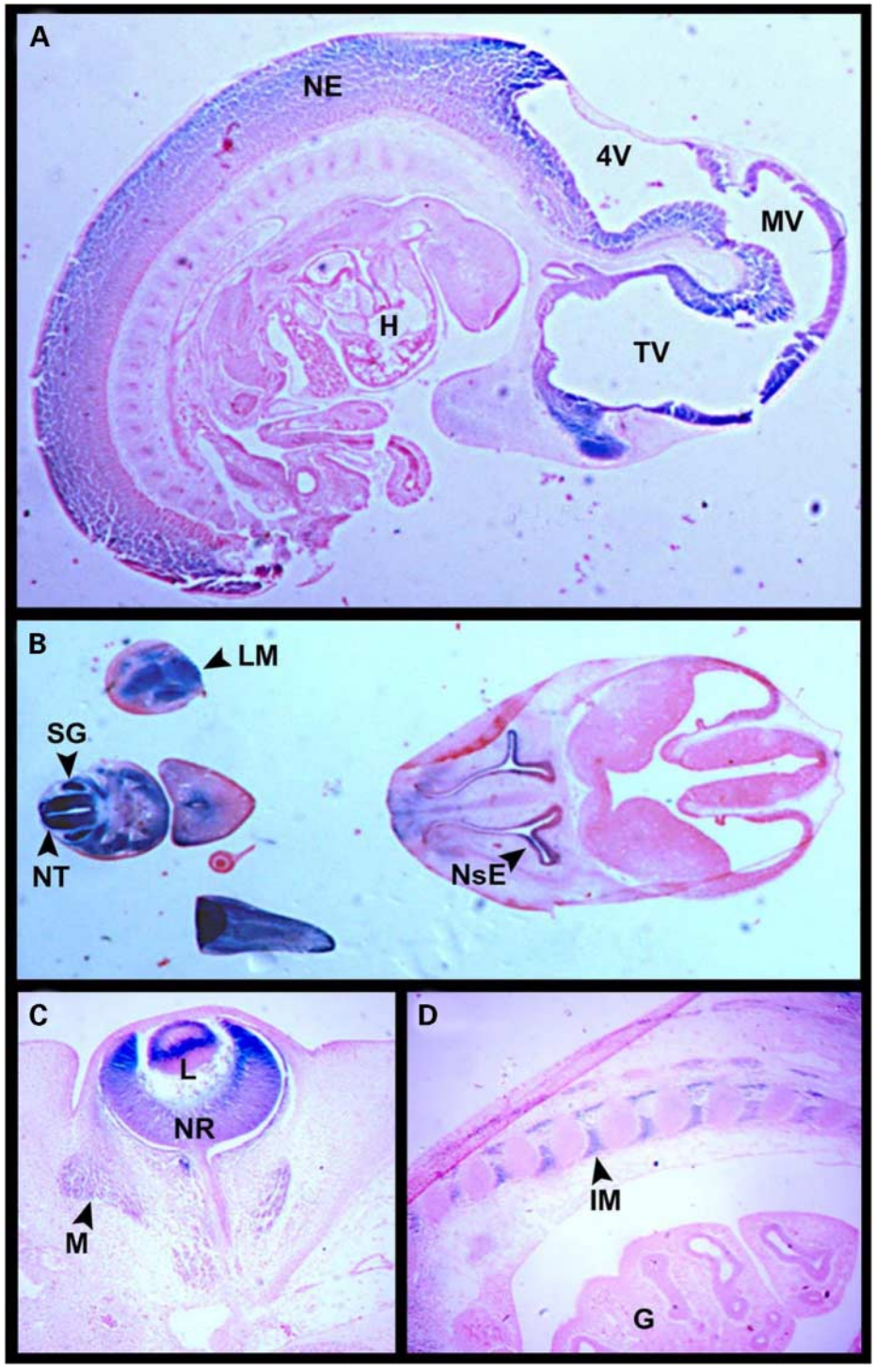

Figure 3. X-gal staining of 11.5 day *Cecr2*$^{+/Gt45Bic}$ embryo sagittal section (**A**) and 13.5 day non-exencephalic *Cecr2*$^{Gt45Bic/Gt45Bic}$ embryo transverse sections (**B**–**D**), showing expression of *Cecr2*. NE, neuroepithelium; 4V, fourth ventricle; MV, mesencephalic ventricle; TV, telencephalic ventrical; H, heart; NT, neural tube; SG, spinal ganglion; LM, limb mesenchyme; NsE, nasal epithelium; L, lens; NR, neuroretina; M, ocular muscle; IM, intercostal mesenchyme; G, gut.

in the absence of substrate we note an absence of ATPase activity in all fractions. The addition of DNA could not stimulate the ATPase activity of CERF; however, nucleosomes are able to stimulate the CERF ATPase activity almost 3-fold over buffer or DNA. Neither vehicle nor mock IP demonstrated any ATPase activity under these conditions, confirming a lack of background ATPase activity. We conclude that, like hNURF, CERF is a nucleosome-dependent ATPase.

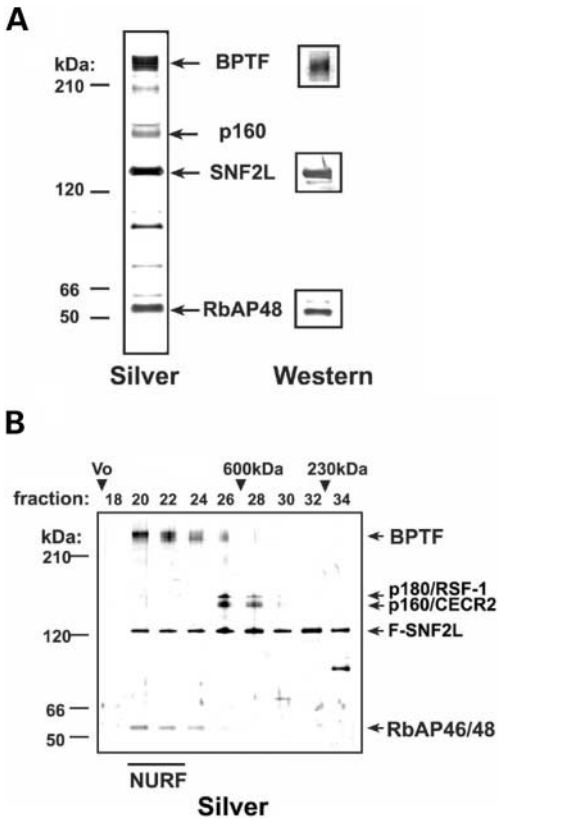

Figure 4. Identification of a novel SNF2L-associated complex. (**A**) Silver stain (left) and western blot (right) of bound SNF2L-associated polypeptides. BPTF, SNF2L, RbAP48 and unknown p160 and p180 polypeptides are indicated. (**B**) Fractions from BioSil Sec400 column were subjected to SDS–PAGE and silver stain analysis. hNURF eluted in fractions 20–24. Fraction number and predicted molecular weights are indicated across the top.

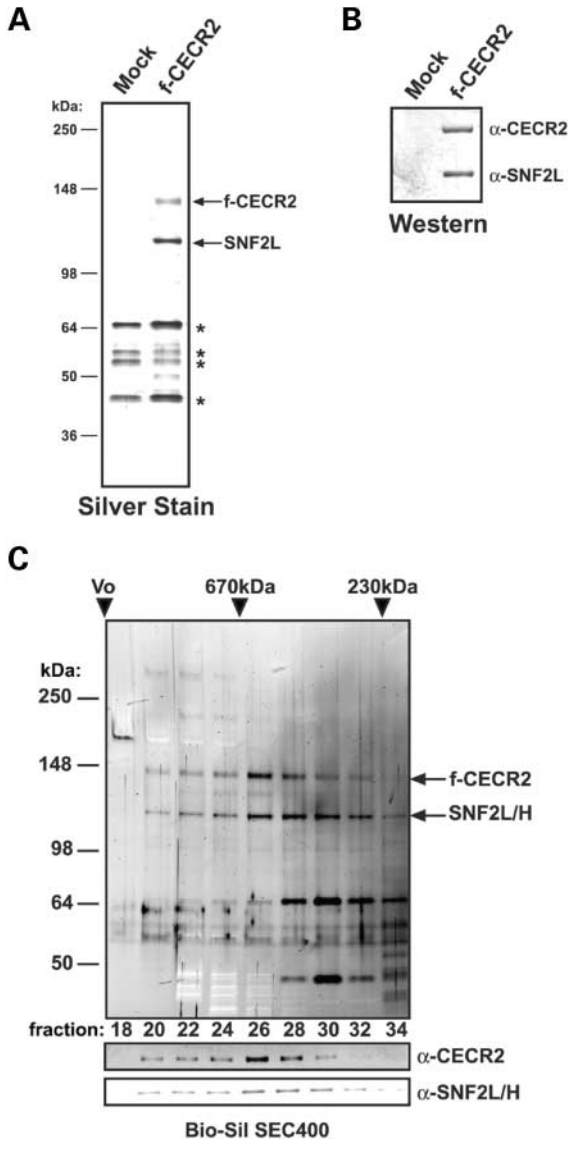

Figure 5. Analysis of the CERF complex. (**A**) Silver stain and (**B**) western blot analysis of naive and Flag-CECR2 HEK293 immunoprecipitates. Nuclear extract from HEK293 cells stably expressing Flag-CECR2 or mock transfected was subjected to anti-Flag immunoaffinity chromatography followed by stringent washes and Flag-peptide-mediated elution of bound proteins. Bound fractions were separated by SDS–PAGE on a 4–12% gel followed by silver stain analysis and western blot. Specific Flag-CECR2-associated polypeptides are labeled to the right. Polypeptides present in both the mock and Flag-CECR2 are marked accordingly (asterisk). Antibodies utilized for immunoblot are indicated. (**C**) CERF purified as in (A) was subjected to molecular weight analysis by size exclusion chromatography on a BioSil SEC400 column. Column fractions were analyzed by silver stain (top) and western blot (bottom) with indicated antibodies. The peak of the CERF complex elutes in fraction 26 corresponding to a molecular weight of ~600 kDa matches well with the purification of CERF complex via the SNF2L subunit (Fig. 4).

CERF is an ATP-dependent chromatin remodeler

ISWI family chromatin remodelers, as their name would imply, are able to remodel chromatin *in vitro.* To assay for this activity in CERF, we utilized the restriction endonuclease coupled chromatin remodeling assay. For this assay, a DNA fragment encoding an array of 5S nucleosome incorporation repeats and a restriction enzyme site at its midpoint is subjected to chromatinization. The incorporated nucleosomes protect the restriction site from its cognate restriction enzyme. These nucleosomes can subsequently be shifted by an ATP-dependent chromatin remodeler thus exposing the restriction enzyme site. This assay measures chromatin remodeling as a function of increased digestion of the chromatinized fragment of DNA. A decrease in the uncut DNA in an ATP-dependent manner indicates chromatin remodeling events (43).

We subjected the chromatinized fragment of DNA to increasing concentrations of the CERF complex. At 30 fmol of CERF, we note potent chromatin remodeling activity as indicated by the decrease in the uncut (U) band. This activity is more pronounced with increasing CERF (Fig. 6B, top). In the absence of ATP (Fig. 6B, bottom), chromatin remodeling activity is undetectable, confirming the specificity of the reaction. Quantification of bands demonstrates the dose dependence of this chromatin remodeling reaction (Fig. 6C). We conclude that, like other ISWI complexes, CERF is capable of remodeling chromatin *in vitro* in an ATP-dependent manner.

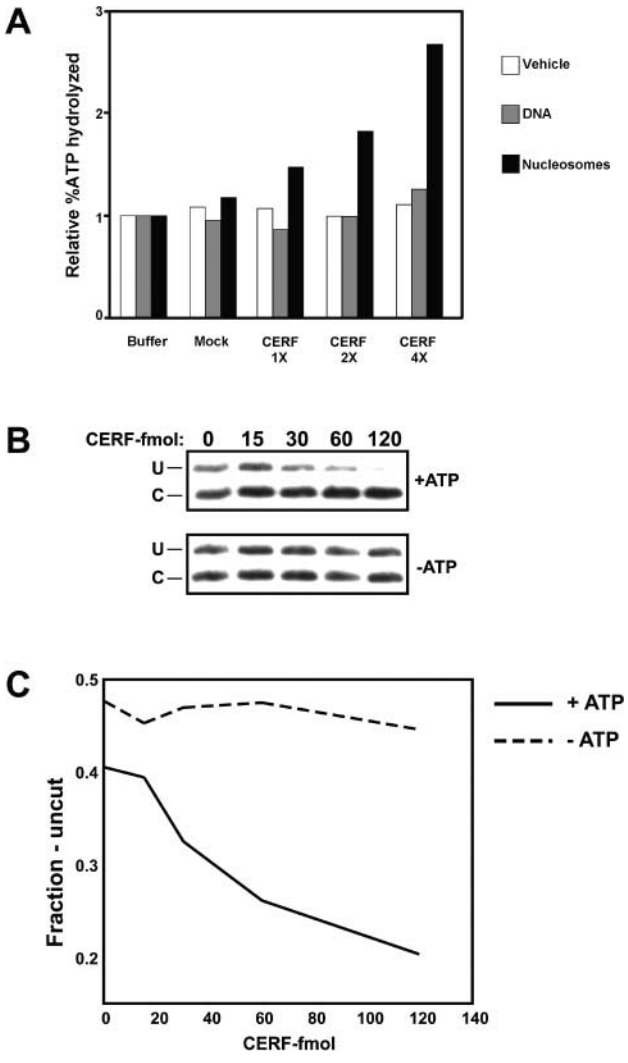

Figure 6. (**A**) CERF displays nucleosome-dependent ATPase and chromatin remodeling activity. Buffer, mock IP or increasing concentrations of CERF were incubated with radiolabeled ATP and indicated substrate: buffer, 250 ng DNA, 250 ng nucleosomes. Reactions were spotted on PEI-cellulose plates and subjected to TLC. Plates were exposed to phosphorimager screens followed by densitometric analysis. We found dose-dependent CERF-mediated ATPase activity only in the presence of nucleosomes. (**B**) Purified CERF was assayed for chromatin remodeling activity utilizing the restriction enzyme coupled chromatin remodeling (RECCR) assay. Autoradiograph of RECCR assay following titration of CERF complex (0, 15, 30, 60 and 120 fmol) with ATP (top) or without ATP (bottom). Chromatin remodeling is indicated by a decrease in the uncut (U) band and an increase in the cut (C) band. (**C**) Graphical display of part (B). Autoradiograph was quantified by densitometry. Points represent the fraction-uncut (U/C + U). Note the CERF dose-dependent decrease in the fraction-uncut in an ATP-dependent manner indicating chromatin remodeling activity.

DISCUSSION

Using a mouse model system and biochemical methods, we have furthered the understanding of *CECR2/Cecr2* with regard to its activities both *in vivo* and *in vitro*. To this end, we describe a mouse mutated for *Cecr2*, which exhibits a profound NTD. In addition, we purified a CECR2-containing complex, CERF, which harbors potent ATPase and chromatin remodeling activity due the association of the chromatin remodeling protein, SNF2L.

NTDs are the second most common birth defect in humans, with a frequency of ~1/1000 births (44). The etiology of NTDs is complex, with both environmental and genetic factors involved. Multiple genes are predicted to be involved in human NTDs and mutations in these genes could act as susceptibility factors. Over 80 genes of widely differing function have been shown to cause NTDs in mice (reviewed in 33) and these genes have become candidates for susceptibility genes in humans. Little is known about how these many genes interact or are regulated.

The phenotype of the mouse mutant for *Cecr2* implicates this gene in regulation of neurulation. BALB/c and 129P2/Ola mice homozygous for $Cecr2^{Gt45Bic}$ develop the NTD exencephaly (the human equivalent to anencephaly) with high penetrance. By inference, this suggests that Snf2l and the CERF complex are involved in the neurulation process.

CECR2/Cecr2 have conserved complex alternative splicing and polyadenylation, suggesting biological relevance (Fig. 1A). The genetrap is located within intron 7, which is present in only some isoforms. If there is transcriptional read-through the genetrap and splicing occurs, only some isoforms may be affected by the genetrap whereas others will be normal. It is possible, therefore, that $Cecr2^{Gt45Bic}$ involves the loss of a specific isoform(s) that is involved in neurulation, perhaps one that retains exons 2–7 and may only be present at a specific time. This would suggest tissue specificity and functional differentiation of the various isoforms. The fact that expression of *CECR2*/*Cecr2* is present in a number of neural and non-neural tissues in embryonic and adult animals (Figs 2 and 3 and data not shown), yet the genetrap mutation only affects neurulation, would support this hypothesis. Analysis of the isoforms in embryos of different ages and genotypes may clarify this.

Variable penetrance for mutations on different mouse strain backgrounds is not uncommon (37,38,45,46). For instance, loss of the proto-oncogene *Ski* results in 83% exencephaly and 0% facial clefting on a 129P2 background, but 5–6% exencephaly and 87–93% facial clefting on a pure C57BL/6J background (37). The mutant *curly tail* shows 18.5% NTDs on a C57BL/6J background, but only 2.2% on a DBA/2 background (reviewed in 45). Mice heterozygous for an AP-2α mutation do not show exencephaly on a 129/SvJae background or when crossed with BALB/c; however, they show 14% exencephaly when crossed to a 129/Ola background (46). There is a striking strain difference in the penetrance of exencephaly with the $Cecr2^{Gt45Bic}$ mutation, showing penetrance of 74% on BALB/c, 63% on 129P2/Ola and 0% on FVB/N. By intercrossing these mutant strains one could search for modifier loci involved in neurulation. Different mouse strains have been shown to have different susceptibility to NTDs (38,47), which is based on strain variation in the position and timing of the initiation of neural tube closure.

Our original interest in *CECR2* was based on its location in the cat eye syndrome critical region. Cat eye syndrome is caused by a duplication of the genes in this region, and as such the *Cecr2* genetrap mutant is unlikely to be directly related to this syndrome. However, underexpression or overexpression might be expected to affect the same tissues and

may cause similar phenotype, as seen in humans with duplications and deletions of 17p12 (48) and 22q11.2 (49). There are no NTDs known to be associated with cat eye syndrome. However, since *CECR2/Cecr2* is expressed in other tissues associated with cat eye syndrome defects, particularly during later brain development and in the eye, and since the genetrap mutation is not a simple loss of function, it is not possible to rule out *CECR2* as a candidate gene for cat eye syndrome.

We have shown that CECR2 functions with SNF2L in a chromatin remodeling complex. In a similar fashion to hNURF, CERF remodels chromatin via a nucleosome-dependent ATPase activity. The localization of Cecr2 to mostly neural structures in the mouse embryo and the characterization of a *Cecr2*^{Gt45Bic} mutation that results in exencephaly suggest that CERF is also involved in neural development. SNF2L has been previously associated with promoting neurite outgrowth in culture (23). This activity was attributed to the hNURF ISWI complex, but the possibility now exists that differentiation and maturation of neurons during development may involve CERF as well as NURF. Through its chromatin remodeling activity, CERF may play a pivotal role in regulating the neurulation pathway.

MATERIALS AND METHODS

RT–PCR and northern hybridizations

RT–PCR was performed using the Thermoscript RT–PCR system (Invitrogen) on placenta mRNA according to the manufacturer's instructions. Northern blots (Clontech) were hybridized according to the manufacturer's instructions using *CECR2* probes ^{32}P-labeled with the Strip-EZ system (Ambion).

Generation and genotyping of *Cecr2*^{Gt45Bic} mice

The mouse ES cell line CT45 (32) containing the β-geo splicetrap vector, pGT1 (50), within *Cecr2* was obtained from Dr Wendy Bickmore (MRC Human Genetics Unit, Edinburgh). CT45 ES cells were grown on plates pretreated with 0.1% gelatin in DMEM with 2 mM L-glutamine, 100 μM β-mercaptoethanol, 0.1 mM MEM non-essential amino acids solution (Invitrogen), 200 μg/ml G418, 1000 U/ml LIF, 15% fetal calf serum (Wysent), 100 U/ml penicillin and 100 μg/ml streptomycin. G418-resistant CT45 ES cells (129P2/Ola) were used for blastocyst injection into C57BL/6J blastocysts. Germline transmission was achieved by mating chimeric male mice to wild-type BALB/c females. Intercrossing the F_1 heterozygotes generated 129P2/BALB mixed background offspring. Incipient congenic BALB/c and FVB/n offspring were generated by intercrossing heterozygotes after five to six backcross generations to the appropriate strain.

Mice were PCR genotyped from DNA extracted from tail clippings or extra-embryonic membranes. A multiplex PCR reaction was utilized, containing two *Cecr2* intron 7 specific primers (7i.F1: 5′-ggcccatgctgttccttcctgatag-3′ and 7i.R1: 5′-aaggctgacattgtgagggcgaaa-3′) one pGT1 genetrap specific primer (pGT1.R4: 5′-acgccatacagtcctcttcacatc-3′) and two male specific *Sry* primers (*Sry* fwd: 5′-gagagcatggagggccat-3′ and *Sry* rev: 5′-ccactcctctgtgacact-3′) for sexing.

Histology

For X-gal staining, embryos were fixed for at least 1 h in 4% paraformaldehyde/PBS at 4°C. Fixed embryos were then rinsed in PBS three times for 5 min each, followed by three washes of 30 min each in LacZ wash solution (1× PBS pH 7.2, 2 mM $MgCl_2$, 0.01% deoxycholic acid, 0.02% IGEPAL). The embryos were then stained in X-gal stain solution (1× PBS pH 7.2, 2 mM $MgCl_2$, 0.01% deoxycholic acid, 0.02% IGEPAL, 5 mM potassium ferricyanide, 5 mM potassium ferrocyanide, 1 mg/ml X-gal) at 37°C until the desired staining intensity was reached (several hours to overnight). After staining, embryos were washed twice for 5 min each in PBS and then dehydrated through a methanol gradient.

For cartilage staining, embryos were fixed for a minimum of 2 h in Bouin's fixative (53% ethanol, 10% formaldehyde, 6.7% glacial acetic acid, 0.45% w/v picric acid). Following fixation, embryos were stained with Alcian blue as described (51), followed by clearing solution (two parts benzyl benzoate, one part benzyl alcohol).

Mammalian cell culture and transfection

HEK293 cells were maintained in DMEM supplemented with 10% FBS, L-glutamine and antibiotics and grown at 37°C with 5% CO_2. HEK293 cells were transfected with FuGene6 (Roche, USA) according to manufacturer's instructions. For stable cell line generation, cells were co-transfected with the cDNA of choice along with a puromycin expressing plasmid for 48 h and transferred to selective media, complete DMEM supplemented with puromycin (2.5 μg/ml). Puromycin resistant colonies were selected, amplified and screened for cDNA expression.

Immunoblot analysis and antibodies

Proteins were separated by 4–12% gradient Tris–glycine SDS–PAGE (Invitrogen) and transferred to PVDF membranes in transfer buffer (50 mM Tris–HCl, 380 mM glycine and 10% methanol). Blots were probed with primary antibodies in Tris-buffered saline containing 0.15% Tween-20, followed by alkaline phosphatase (AP)-conjugated anti-rabbit antibodies (Promega, USA). All blots were visualized as described (52). Anti-CECR2 polyclonal antibodies were raised against a KLH-conjugated peptide corresponding to amino acids 1443–1464 of CECR2. Anti-Flag antibodies were purchased from Sigma, USA. Anti-RbAP48 monoclonal antibodies were purchased from Upstate, USA. Anti-RbAP46 and anti-RbAP46 polyclonal antibodies were purchased from Oncogene, USA.

Mass spectrometric peptide sequencing

Excised bands were subjected to N-terminal sequence analysis as described (17).

Restriction endonuclease coupled remodeling assay

Twenty microliter reactions containing 10 mM Tris–HCl (pH 7.9), 125 mM KCl, 1 mM ATP, 2.5 mM $MgCl_2$, 1 mM DTT, 2.5% glycerol, 100 μg/ml BSA, 0.5 μl HC-*Sal* I (NEB), 0.5 μl of nucleosomal array along with varying amounts of Flag purified CERF or mock elutions, where indicated, were

incubated for 90 min at 37°C. The DNA array was then deproteinated by phenol/chloroform extraction. Aqueous fractions containing DNA were supplemented with DNA sample buffer followed by electrophoresis on a 1% agarose gel. The gel was placed on a sheet of DE81 chromatography paper (Whatman) and dried under vacuum for 2 h at 60°C. The dried gel was then analyzed by phosphoimager (Molecular Dynamics), and bands were quantified by densitometric analysis.

ATPase assays

Measurement of ATPase activity was performed in 10 μl reactions under the following conditions: 20 mM Tris–HCl, 60 mM KCl, 4% glycerol, 4 mM $MgCl_2$, 1 mM cold ATP, 1 μCi [γ^{32}-P] ATP and 2 nmol of CERF or an equivalent volume of elution buffer. Where indicated, the reaction was supplemented with 50 ng of naked DNA or nucleosomes. Reactions were performed at 30°C for 1 h. Free phosphate and ATP, were separated by thin layer chromatography (TLC) on PEI-cellulose plates (J.T. Baker, USA). One microliter of reaction was spotted on the plate and TLC was carried out in 1 M formic acid, 0.5 M LiCl. Plates were then allowed to dry and were visualized by exposure to phosphorimager cassette (Molecular Dynamics, Sweden) for densitometric analysis or film (Kodak, USA).

Purification of SNF2L-associated complexes

Nuclear extracts were prepared from stable Flag-SNF2L HEK293 cells according to a previously published protocol (53). Extracts were subjected to dialysis against BC buffer (20 mM Tris–HCl, 10% glycerol, 0.2 mM EDTA, pH 7.8) supplemented with 100 mM KCl and protease inhibitors. Complexes were immunoprecipitated from dialyzed extract overnight. Beads were washed in three consecutive 10 column volume washes containing BC500 supplemented with 0.5% NP-40, BC750 supplemented with 0.1% NP-40 and BC1000 supplemented with 0.1% NP-40. Finally, beads were rinsed in BC100 and subjected to 5–1 column volume elutions using BC100 supplemented with 400 μg/ml of Flag peptide (Sigma). Immunoprecipitates were analyzed by SDS–PAGE followed by silver stain and immunoblot for SNF2L and known associated polypeptides.

Size exclusion chromatography

Recombinant Flag-SNF2L + 13 or stable cell line immunoprecipitations were fractionated using a BioSil Sec400 gel filtration column (BioRad) equilibrated in BC500 supplemented with 0.1% NP-40 and protease inhibitors. Using SDS–PAGE, 0.3 ml fractions were analyzed, followed by immunoblot for SNF2L.

ACKNOWLEDGEMENTS

We would like to thank Dr Wendy Bickmore for providing the ES genetrap cell line CT-45, Dr Peter Dickie for expertise with ES cell injections and the Wistar Institute protein microchemistry/mass spectrometry facility. R.S. was supported by grants from NIH (GM61204) and the American Cancer Society. H.E.M. was supported by grants from the Canadian Institutes of Health Research (MOP11639 and MOP64361). O.G.B. was supported by the NIH cancer grant (CA09171-28).

REFERENCES

1. Aalfs, J.D. and Kingston, R.E. (2000) What does 'chromatin remodeling' mean? *Trends Biochem. Sci.*, **25**, 548–555.
2. Lusser, A. and Kadonaga, J.T. (2003) Chromatin remodeling by ATP-dependent molecular machines. *Bioessays*, **25**, 1192–1200.
3. Ausio, J., Levin, D.B., De Amorim, G.V., Bakker, S. and Macleod, P.M. (2003) Syndromes of disordered chromatin remodeling. *Clin. Genet.*, **64**, 83–95.
4. Hendrich, B. and Bickmore, W. (2001) Human diseases with underlying defects in chromatin structure and modification. *Hum. Mol. Genet.*, **10**, 2233–2242.
5. Gibbons, R.J., Pellagatti, A., Garrick, D., Wood, W.G., Malik, N., Ayyub, H., Langford, C., Boultwood, J., Wainscoat, J.S. and Higgs, D.R. (2003) Identification of acquired somatic mutations in the gene encoding chromatin-remodeling factor ATRX in the alpha-thalassemia myelodysplasia syndrome (ATMDS). *Nat. Genet.*, **34**, 446–449.
6. Picketts, D.J., Higgs, D.R., Bachoo, S., Blake, D.J., Quarrell, O.W. and Gibbons, R.J. (1996) ATRX encodes a novel member of the SNF2 family of proteins: mutations point to a common mechanism underlying the ATR-X syndrome. *Hum. Mol. Genet.*, **5**, 1899–1907.
7. Sun, L.Q., Lee, D.W., Zhang, Q., Xiao, W., Raabe, E.H., Meeker, A., Miao, D., Huso, D.L. and Arceci, R.J. (2004) Growth retardation and premature aging phenotypes in mice with disruption of the SNF2-like gene, *PASG. Genes Dev.*, **18**, 1035–1046.
8. Badenhorst, P., Voas, M., Rebay, I. and Wu, C. (2002) Biological functions of the ISWI chromatin remodeling complex NURF. *Genes Dev.*, **16**, 3186–3198.
9. Deuring, R., Fanti, L., Armstrong, J.A., Sarte, M., Papoulas, O., Prestel, M., Daubresse, G., Verardo, M., Moseley, S.L., Berloco, M. *et al.* (2000) The ISWI chromatin-remodeling protein is required for gene expression and the maintenance of higher order chromatin structure *in vivo*. *Mol. Cell*, **5**, 355–365.
10. Tsukiyama, T., Daniel, C., Tamkun, J. and Wu, C. (1995) ISWI, a member of the SWI2/SNF2 ATPase family, encodes the 140 kDa subunit of the nucleosome remodeling factor. *Cell*, **83**, 1021–1026.
11. Ito, T., Bulger, M., Pazin, M.J., Kobayashi, R. and Kadonaga, J.T. (1997) ACF, an ISWI-containing and ATP-utilizing chromatin assembly and remodeling factor. *Cell*, **90**, 145–155.
12. Varga-Weisz, P.D., Wilm, M., Bonte, E., Dumas, K., Mann, M. and Becker, P.B. (1997) Chromatin-remodelling factor CHRAC contains the ATPases ISWI and topoisomerase II. *Nature*, **388**, 598–602.
13. Aihara, T., Miyoshi, Y., Koyama, K., Suzuki, M., Takahashi, E., Monden, M. and Nakamura, Y. (1998) Cloning and mapping of SMARCA5 encoding hSNF2H, a novel human homologue of Drosophila ISWI. *Cytogenet. Cell. Genet.*, **81**, 191–193.
14. Lazzaro, M.A. and Picketts, D.J. (2001) Cloning and characterization of the murine Imitation Switch (ISWI) genes: differential expression patterns suggest distinct developmental roles for Snf2h and Snf2l. *J. Neurochem.*, **77**, 1145–1156.
15. Okabe, I., Bailey, L.C., Attree, O., Srinivasan, S., Perkel, J.M., Laurent, B.C., Carlson, M., Nelson, D.L. and Nussbaum, R.L. (1992) Cloning of human and bovine homologs of SNF2/SWI2: a global activator of transcription in yeast *S. cerevisiae*. *Nucleic Acids Res.*, **20**, 4649–4655.
16. Stopka, T. and Skoultchi, A.I. (2003) The ISWI ATPase Snf2h is required for early mouse development. *Proc. Natl Acad. Sci. USA*, **100**, 14097–14102.
17. Bochar, D.A., Savard, J., Wang, W., Lafleur, D.W., Moore, P., Cote, J. and Shiekhattar, R. (2000) A family of chromatin remodeling factors related to Williams' syndrome transcription factor. *Proc. Natl Acad. Sci. USA*, **97**, 1038–1043.
18. LeRoy, G., Orphanides, G., Lane, W.S. and Reinberg, D. (1998) Requirement of RSF and FACT for transcription of chromatin templates *in vitro*. *Science*, **282**, 1900–1904.

19. Bozhenok, L., Wade, P.A. and Varga-Weisz, P. (2002) WSTF-ISWI chromatin remodeling complex targets heterochromatic replication foci. *EMBO J.*, **21**, 2231–2241.
20. Strohner, R., Nemeth, A., Jansa, P., Hofmann-Rohrer, U., Santoro, R., Langst, G. and Grummt, I. (2001) NoRC—a novel member of mammalian ISWI-containing chromatin remodeling machines. *EMBO J.*, **20**, 4892–4900.
21. Poot, R.A., Dellaire, G., Hulsmann, B.B., Grimaldi, M.A., Corona, D.F., Becker, P.B., Bickmore, W.A. and Varga-Weisz, P.D. (2000) HuCHRAC, a human ISWI chromatin remodelling complex contains hACF1 and two novel histone-fold proteins. *EMBO J.*, **19**, 3377–3387.
22. Hakimi, M.A., Bochar, D.A., Schmiesing, J.A., Dong, Y., Barak, O.G., Speicher, D.W., Yokomori, K. and Shiekhattar, R. (2002) A chromatin remodelling complex that loads cohesin onto human chromosomes. *Nature*, **418**, 994–998.
23. Barak, O., Lazzaro, M.A., Speicher, D.W., Picketts, D.J. and Shiekhattar, R. (2003) Isolation of human NURF: a regulator of engrailed gene expression. *EMBO J.*, **22**, 6089–6100.
24. Wurst, W., Auerbach, A.B. and Joyner, A.L. (1994) Multiple developmental defects in Engrailed-1 mutant mice: an early mid-hindbrain deletion and patterning defects in forelimbs and sternum. *Development*, **120**, 2065–2075.
25. Millen, K.J., Hui, C.C. and Joyner, A.L. (1995) A role for En-2 and other murine homologues of Drosophila segment polarity genes in regulating positional information in the developing cerebellum. *Development*, **121**, 3935–3945.
26. Footz, T.K., Brinkman-Mills, P., Banting, G.S., Maier, S.A., Riazi, M.A., Bridgland, L., Hu, S., Birren, B., Minoshima, S., Shimizu, N. *et al.* (2001) Analysis of the cat eye syndrome critical region in humans and the region of conserved synteny in mice: a search for candidate genes at or near the human chromosome 22 pericentromere. *Genome Res.*, **11**, 1053–1070.
27. Liu, L. and McKeehan, W.L. (2002) Sequence analysis of LRPPRC and its SEC1 domain interaction partners suggests roles in cytoskeletal organization, vesicular trafficking, nucleocytosolic shuttling, and chromosome activity. *Genomics*, **79**, 124–136.
28. Fyodorov, D.V. and Kadonaga, J.T. (2002) Binding of Acf1 to DNA involves a WAC motif and is important for ACF-mediated chromatin assembly. *Mol. Cell. Biol.*, **22**, 6344–6353.
29. Zeng, L. and Zhou, M.M. (2002) Bromodomain: an acetyl-lysine binding domain. *FEBS Lett.*, **513**, 124–128.
30. Hassan, A.H., Prochasson, P., Neely, K.E., Galasinski, S.C., Chandy, M., Carrozza, M.J. and Workman, J.L. (2002) Function and selectivity of bromodomains in anchoring chromatin-modifying complexes to promoter nucleosomes. *Cell*, **111**, 369–379.
31. Agalioti, T., Chen, G. and Thanos, D. (2002) Deciphering the transcriptional histone acetylation code for a human gene. *Cell*, **111**, 381–392.
32. Tate, P., Lee, M., Tweedie, S., Skarnes, W.C. and Bickmore, W.A. (1998) Capturing novel mouse genes encoding chromosomal and other nuclear proteins. *J. Cell Sci.*, **111**, 2575–2585.
33. Copp, A.J., Greene, N.D. and Murdoch, J.N. (2003) The genetic basis of mammalian neurulation. *Nat. Rev. Genet.*, **4**, 784–793.
34. Nottoli, T., Hagopian-Donaldson, S., Zhang, J., Perkins, A. and Williams, T. (1998) AP-2-null cells disrupt morphogenesis of the eye, face, and limbs in chimeric mice. *Proc. Natl Acad. Sci. USA*, **95**, 13714–13719.
35. Winograd, J., Reilly, M.P., Roe, R., Lutz, J., Laughner, E., Xu, X., Hu, L., Asakura, T., vander Kolk, C., Strandberg, J.D. *et al.* (1997) Perinatal lethality and multiple craniofacial malformations in MSX2 transgenic mice. *Hum. Mol. Genet.*, **6**, 369–379.
36. Barbera, J.P., Rodriguez, T.A., Greene, N.D., Weninger, W.J., Simeone, A., Copp, A.J., Beddington, R.S. and Dunwoodie, S. (2002) Folic acid prevents exencephaly in Cited2 deficient mice. *Hum. Mol. Genet.*, **11**, 283–293.
37. Colmenares, C., Heilstedt, H.A., Shaffer, L.G., Schwartz, S., Berk, M., Murray, J.C. and Stavnezer, E. (2002) Loss of the SKI proto-oncogene in individuals affected with 1p36 deletion syndrome is predicted by strain-dependent defects in Ski−/− mice. *Nat. Genet.*, **30**, 106–109.
38. Fleming, A. and Copp, A.J. (2000) A genetic risk factor for mouse neural tube defects: defining the embryonic basis. *Hum. Mol. Genet.*, **9**, 575–581.
39. Loyola, A., Huang, J.Y., LeRoy, G., Hu, S., Wang, Y.H., Donnelly, R.J., Lane, W.S., Lee, S.C. and Reinberg, D. (2003) Functional analysis of the subunits of the chromatin assembly factor RSF. *Mol. Cell. Biol.*, **23**, 6759–6768.
40. Collins, N., Poot, R.A., Kukimoto, I., Garcia-Jimenez, C., Dellaire, G. and Varga-Weisz, P.D. (2002) An ACF1-ISWI chromatin-remodeling complex is required for DNA replication through heterochromatin. *Nat. Genet.*, **32**, 627–632.
41. Shamay, M., Barak, O., Doitsh, G., Ben-Dor, I. and Shaul, Y. (2002) Hepatitis B virus pX interacts with HBXAP, a PHD finger protein to coactivate transcription. *J. Biol. Chem.*, **277**, 9982–9988.
42. Aalfs, J.D., Narlikar, G.J. and Kingston, R.E. (2001) Functional differences between the human ATP-dependent nucleosome remodeling proteins BRG1 and SNF2H. *J. Biol. Chem.*, **276**, 34270–34278.
43. Logie, C. and Peterson, C.L. (1997) Catalytic activity of the yeast SWI/SNF complex on reconstituted nucleosome arrays. *EMBO J.*, **16**, 6772–6782.
44. Campbell, L.R., Dayton, D.H. and Sohal, G.S. (1986) Neural tube defects: a review of human and animal studies on the etiology of neural tube defects. *Teratology*, **34**, 171–187.
45. van Straaten, H.W. and Copp, A.J. (2001) Curly tail: a 50-year history of the mouse spina bifida model. *Anat. Embryol.* (*Berl*), **203**, 225–237.
46. Kohlbecker, A., Lee, A.E. and Schorle, H. (2002) Exencephaly in a subset of animals heterozygous for AP-2alpha mutation. *Teratology*, **65**, 213–218.
47. Juriloff, D.M., Harris, M.J., Tom, C. and MacDonald, K.B. (1991) Normal mouse strains differ in the site of initiation of closure of the cranial neural tube. *Teratology*, **44**, 225–233.
48. Lupski, J.R. (1998) Charcot-Marie-Tooth disease: lessons in genetic mechanisms. *Mol. Med.*, **4**, 3–11.
49. Ensenauer, R.E., Adeyinka, A., Flynn, H.C., Michels, V.V., Lindor, N.M., Dawson, D.B., Thorland, E.C., Lorentz, C.P., Goldstein, J.L., McDonald, M.T. *et al.* (2003) Microduplication 22q11.2, an emerging syndrome: clinical, cytogenetic, and molecular analysis of thirteen patients. *Am. J. Hum. Genet.*, **73**, 1027–1040.
50. Wilson, V., Manson, L., Skarnes, W.C. and Beddington, R.S. (1995) The T gene is necessary for normal mesodermal morphogenetic cell movements during gastrulation. *Development*, **121**, 877–886.
51. Jegalian, B.G. and De Robertis, E.M. (1992) Homeotic transformations in the mouse induced by overexpression of a human Hox3.3 transgene. *Cell*, **71**, 901–910.
52. Harlow, E. and Lane, D. (1988) *Antibodies: A Laboratory Manual.* Cold Spring Harbor Press, Cold Spring Harbor, NY.
53. Dignam, J.D. (1990) Preparation of extracts from higher eukaryotes. *Methods Enzymol.*, **182**, 194–203.